analytical chemistry

Article

pubs.acs.org/ac

Interfacial Self-Assembled Functional Nanoparticle Array: A Facile Surface-Enhanced Raman Scattering Sensor for Specific Detection of Trace Analytes

Kun Zhang, Ji Ji, Yixin Li, and Baohong Liu*

Department of Chemistry, State Key Lab of Molecular Engineering of Polymers and Institutes of Biomedical Sciences, Fudan University, Shanghai 200433, China

Supporting Information

ABSTRACT: Surface-enhanced Raman scattering (SERS) has proven to be promising for the detection of trace analytes; however, the precise nanofabrication of a specific and sensitive plasmonic SERS-active substrate is still a major challenge that limits the scope of its applications. In this work, gold nanoparticles are self-assembled into densely packed two-dimensional arrays at a liquid/liquid interface between dimethyl carbonate and water in the absence of template controller molecules. Both the simulation and experiment results show that the particles within these film-like arrays exhibit strong electromagnetic coupling and enable large amplification of Raman signals. In order to realize the level of sensing specificity, the surface chemistry of gold nanoparticles (Au NPs) is rationally tailored by incorporating an appropriate chemical moiety that specifically captures molecules of interest. The ease of fabrication and good uniformity make this platform ideal for in situ SERS sensing of trace targets in complex samples.

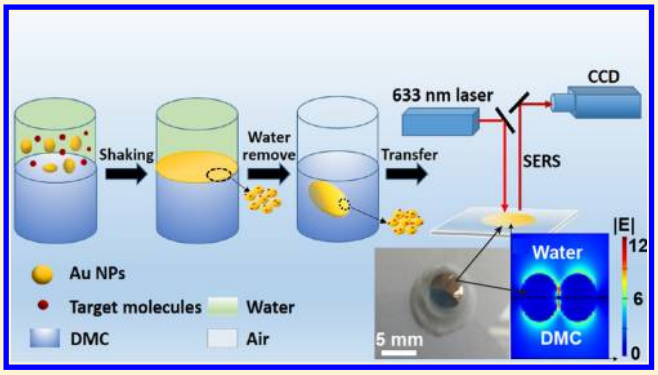

Surface enhanced Raman scattering (SERS) is a powerful vibrational spectroscopic technique that can extend the sensitivity of conventional Raman spectroscopy to the single-molecule level.[1,2] The drastically enhanced signal gives SERS great potential for applications in chemical and biological assays.[3,4] Despite such potential, the development of SERS-based sensors for trace analyte detection remains a challenge, mainly owing to the complication and high cost associated with the preparation of enhancing substrates with controlled nanostructure, well-defined periodicity, and high chemical stability. More importantly, although the intrinsically narrow line widths of Raman bands can reduce spectral overlap and thus improve to some extent the specificity of SERS detection, interference from coexistent species, especially structural analogues of the target molecule, in a complex sample mixture still represents a big problem.

Recent studies have demonstrated that densely arranged two-dimensional (2D) nanoarrays are promising to serve as SERS substrates in terms of sensitivity and reproducibility.[5−8] Several distinct approaches to fabricate such substrates have been reported. Tian and co-workers developed the SERS enhancement based on the monolayer of shell-isolated gold nanoparticles (Au NPs).[9] Van Duyne and co-workers fabricated 2D substrates by using immobilized nanorod assemblies.[10] Other strategies using Langmuir−Blodgett (LB) assembly,[6] vacuum evaporation,[11] and lithography-based techniques such as electron beam lithography,[12] focused ion beam lithography,[7] and nanoimprint lithography[13] have also been studied. Very high enhancements can be achieved by these methods, while some of them involve multistep synthetic processes or a sophisticated apparatus. In this context, a bottom-up strategy relying on self-assembly provides an alternative and convenient way for engineering NPs.[14,15] Among the available self-assembly methods, assembly at liquid/liquid interfaces offers a facile route to generate densely arranged nanostructures driven by minimization of the interfacial energy.[16−22] Recently, the self-assembled NP arrays have been first proposed for multiphase trace detection by Edel's group, where Au NPs were quickly organized at the oil/water interface in the presence of sodium chloride.[23] Similarly, Konrad et al. obtained stable and uniform SERS signals from densely packed Ag NP arrays which were formed at a dichloromethane/water interface by using tetrabutylammonium nitrate as a "promoter" molecule.[24] In this work, we present a dimethyl carbonate (DMC)/water system that can efficiently organize Au NPs at the oil/water interface in the absence of additional controller molecules. DMC with a polarity relatively closer to that of water has been demonstrated to favor the assembly process due to a synergistic effect of the interfacial energy and more interaction with water.[21] The formed interfacial NP arrays were subsequently employed as a

Received: April 16, 2014
Accepted: June 10, 2014
Published: June 10, 2014

 © 2014 American Chemical Society dx.doi.org/10.1021/ac501383x | Anal. Chem. 2014, 86, 6660−6665

simple SERS sensor capable of testing trace analytes in sample mixtures. Both the experimental and simulated results showed that Au NPs within the densely arranged 2D assemblies exhibited intense electromagnetic coupling that created numerous "hot spots" uniformly distributed over the detection area. In order to realize the level of detection specificity, the surface chemistry of Au NPs was rationally tailored by incorporating an appropriate chemical moiety that could specifically capture the molecules of interest. A method for the rapid detection of 2,4,6-trinitrotoluene (TNT) at subfemtomolar levels without interference from its structural analogous was presented to demonstrate the capability of our interfacial assembled SERS sensor.

EXPERIMENTAL SECTION

Materials. Hydrogen tetrachloroaurate ($HAuCl_4 \cdot 3H_2O$) was purchased from Sigma-Aldrich. Trisodium citrate dihydrate ($Na_3C_6O_7 \cdot 2H_2O$), L-cysteine, 2,4,6-trinitrotoluene (TNT), 2,4-dinitrotoluene (DNT), and 3-nitrotoluene (NT) were purchased from Aladdin Reagent (Shanghai, China). Acetonitrile, ethanol absolute, dimethyl carbonate (DMC), 1,2-dichloroethane (DCE), and other chemicals were of analytical grade or better and used without further purification. All solutions and dilutions were prepared using ultrapure water with a resistivity larger than 18.2 MΩcm.

Synthesis of Gold Nanoparticles (Au NPs). Citrate-stabilized Au NPs were synthesized according to Frens' method.[25] Typically, 50 mL of 0.01% $HAuCl_4$ solution was heated to boiling and 0.65 mL of 1% trisodium citrate solution was added to the boiling solution under vigorous stirring. The solution was continually boiled for 5 min to give a red solution. The resulting particles were approximately 30 nm in diameter according to field-emission scanning electron microscopy (FE-SEM) and had an average hydrodynamic diameter of 77.5 ± 44.4 nm with a polydispersity index of 0.352 using dynamic light scattering (DLS). A molar extinction coefficient, ε_{max}, of $(6.06 \pm 0.03) \times 10^9$ $M^{-1}cm^{-1}$ at 532 nm was used to measure the concentration of the particles by UV–vis spectroscopy.[26]

Au NPs Surface Functionalization. The surfaces of the as-prepared Au NPs were modified with cysteine to selectively detect TNT. 0.5 mL of 100 nM L-cysteine solution and 4.5 mL of Au NPs (0.33 nM) were incubated by moderate stirring for 3 h. The modified NPs were isolated by centrifugation and redispersed in water. UV–vis spectroscopy, FE-SEM, and DLS were used to characterize the surface-functionalized NPs.

Self-Assembly of Au NPs at the Liquid/Liquid Interface. The densely packed interfacial arrays were prepared in a 2 mL polypropylene centrifuge tube where 200 μL of Au NPs aqueous solution was vigorously shaken for approximately 10 s with 400 μL of DMC. After shaking, the resulting emulsion rapidly separated into two distinct phases, and a metallic film with a golden reflection formed spontaneously between the two phases. Then, all but 20 μL of water was removed, resulting in an aqueous droplet suspended in the oil that consisted of NPs at the oil/liquid interface.

TNT Detection by Interfacial Assembled Functional NP Arrays. In order to detect TNT using the self-assembled 2D arrays, a 10 μL portion of TNT solution of known concentration (solvent: ethanol/acetonitrile, 8:2, v/v) was premixed with the amine-capped Au NPs colloids. The NPs were then assembled at the DMC/liquid interface with the aforementioned procedures. SERS measurement was scanned from 500 to 3000 cm^{-1}.

Characterizations. FE-SEM was performed with a Nova NanoSEM 230 electron microscope at an accelerating voltage of 3.00 kV. UV–vis spectroscopy was measured on an Agilent HP8453 spectrophotometer. The DLS data was obtained by Zetasizer from Malvern Instruments. SERS spectra were recorded with a Labram-1B Raman spectrometer from Yobin Yvon with a laser (2 mW) excitation wavelength of 632.8 nm. An acquisition time of 5 s per spectrum was used to reduce the influence of evaporation, and the stage position and the optical focus were adjusted manually to probe different positions of the droplet during the course of the measurement.

RESULTS AND DISCUSSION

The proposed method relying on self-assembly of NPs at the liquid/liquid interface is illustrated in Figure 1. After vigorously

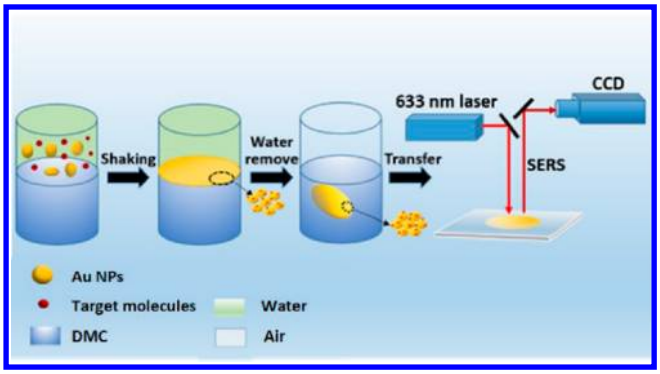

Figure 1. Self-assembly of cysteine-functionalized Au NPs at the DMC/water interface and its application as a SERS sensor for detection of the trace analyte.

shaking a two-phase system consisting of DMC and Au NPs aqueous suspension, the NP assembly with a golden reflection formed spontaneously at the oil/water interface within 1 min. This assembly is dictated by the minimization of the interfacial energy, which is highly dependent on the size of the nanoparticle and the equilibrium contact angle (θ). For a small particle, the energy E required to remove it from the interface is given by[27]

$$E = \pi R^2 \gamma_{o/w} (1 \pm \cos\theta)^2 \quad (1)$$

where R is the radius of the particle, $\gamma_{o/w}$ is the interfacial tension, and θ is the contact angle. The interfacial tension between the immiscible phases can be estimated by[28]

$$\gamma_{o/w} = \gamma_o + \gamma_w - 2(\gamma_o \gamma_w)^{1/2} \quad (2)$$

where γ_o is the surface tension of the oil phase and γ_w is the surface tension of water. Wetting experiments indicated that the contact angle was close to 90° when an interfacial layer of NPs was formed.[29,30] Therefore, according to the reported values for γ_{DMC} of 28.8 mN/m and γ_{water} of 72.88 mN/m, E is estimated to be approximately 1750 kT for the 30 nm Au NPs used in this study, which is considerably larger than the thermal energy, indicating that the particles can stably reside at the interface rather than escape into the liquid. It is worthy of note that no additional controllers such as methanol, ethanol, or salt were employed to promote assembly of NPs at the interface in this protocol. Removing most of the water phase led to the formation of an aqueous droplet suspended in the oil phase. The droplet consisted of concentrated NPs at the liquid/liquid

dx.doi.org/10.1021/ac501383x | Anal. Chem. 2014, 86, 6660–6665

interface and could be readily transferred onto arbitrary substrates such as a glass slide to perform the SERS measurements.

Figure 2A shows a digital photograph of the liquid droplet consisting of the self-assembled NP film. As demonstrated above, the NP film exhibited a uniform and highly reflective golden appearance in reflected light. Figure 2B shows an SEM image of the interfacial assembled NP arrays prepared by transferring the droplet on a piece of indium tin oxide (ITO) glass followed by pipetting the liquid. The image indicated that the dried Au NP arrays were closely packed into a 2D monolayer, although there existed a few vacancies that were caused during transferring the droplet to the glass slide.[21,23] The high density suggested that some clusters were formed at the interface where the Au NPs were in close proximity to their neighbors, which was very beneficial for strong plasmonic coupling and the creation of electromagnetic "hot spots". The monolayer structure ensured that all "hot spots" were confined within the area illuminated by the laser beam. The strong interparticle plasmonic coupling was experimentally confirmed by UV−vis extinction spectroscopy. As shown in Figure 2C, the plasmon peak of the 30 nm Au colloid was at 532 nm, while the assemblies had a decreased peak at 532 nm and a strong broad band at about 830 nm. The theoretical simulation also confirmed the variation of the plasmonic properties when Au NPs were assembled into a monolayer at the oil/water interface. The intensity of the electric field was remarkably enhanced and highly concentrated at the gap region between neighboring NPs after the formation of the interfacial assembly, indicating the intense interparticle electronic coupling (Figure S1, Supporting Information). The result was consistent with previous reports on the localized surface plasmon resonance of the Au NPs assembled at liquid/liquid interfaces.[31,32]

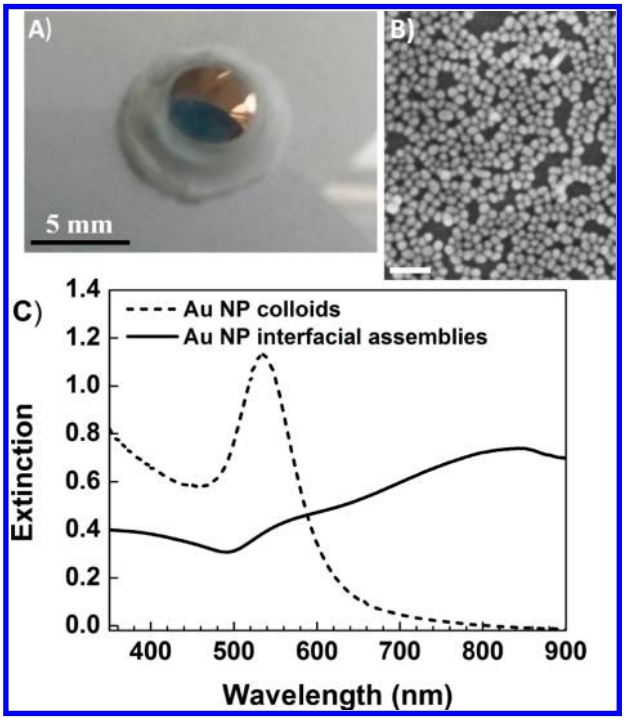

Figure 2. (A) Photograph of the interfacial assembled Au NP arrays formed at the DMC/water interface. The arrays had a golden appearance in reflected light and were blue when viewed in transmission light. (B) FE-SEM image of the self-assemblies which was deposited on a glass slide and then dried. The scale bar was 100 nm. (C) UV−vis extinction spectra of Au NP colloid and the interfacial assemblies of Au NPs.

The spatial uniformity is an important parameter for SERS-active substrates. In order to evaluate the reproducibility of the signal intensity over the interfacial assembled NP arrays, Raman spectra were randomly measured at 15 different spots within the assemblies. Rhodamine 6G (R6G) was used as a Raman reporter because of the resonance effect of this molecule on the Au substrate. A typical spectrum of R6G is shown in Figure 3A.

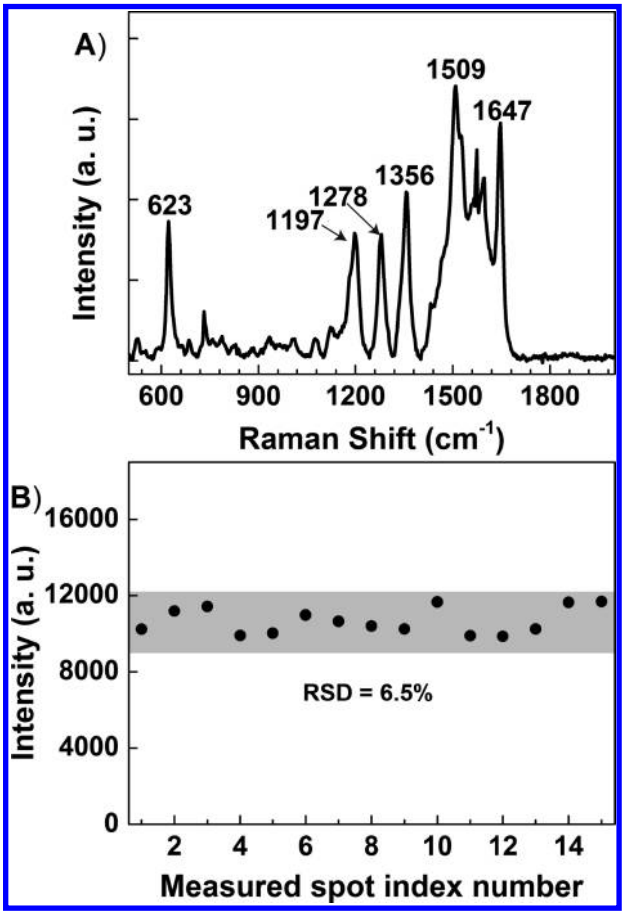

Figure 3. (A) Raman spectrum of rhodamine 6G recorded on the surface of the Au NP assemblies. (B) Intensities of the peak at 1509 cm^{-1} of R6G for 15 spots randomly distributed on the Au NP assemblies.

The marked peaks were all corresponding to the Raman lines for R6G.[33] The most prominent band was at about 1509 cm^{-1}, and the relative standard deviation was 6.5% (Figure 3B). This value is comparable to or better than those previously reported results of NP assemblies, suggesting the desirable spatial uniformity of our interfacial arrays.[34−39]

DMC was chosen as the organic phase for interfacial assembly of Au NPs in this study. There are several advantages of this solvent. The properties of nontoxicity and biodegradability make DMC a safe, secure, and environment-friendly solvent.[40,41] More importantly, although the two phases are immiscible, water in fact has a certain solubility in DMC (up to 2.9% in weight). Hence, the droplet would subsequently experience shrinkage that further increases the particle density at the liquid−liquid interface.[42] Compared with 1,2-dichloroethane (DCE), a commonly used oil phase for NPs assembly,

dx.doi.org/10.1021/ac501383x | Anal. Chem. 2014, 86, 6660−6665

the DMC/water interface exhibited much higher efficiency to adsorb and organize Au NPs. As shown in Figure 4B, a closely

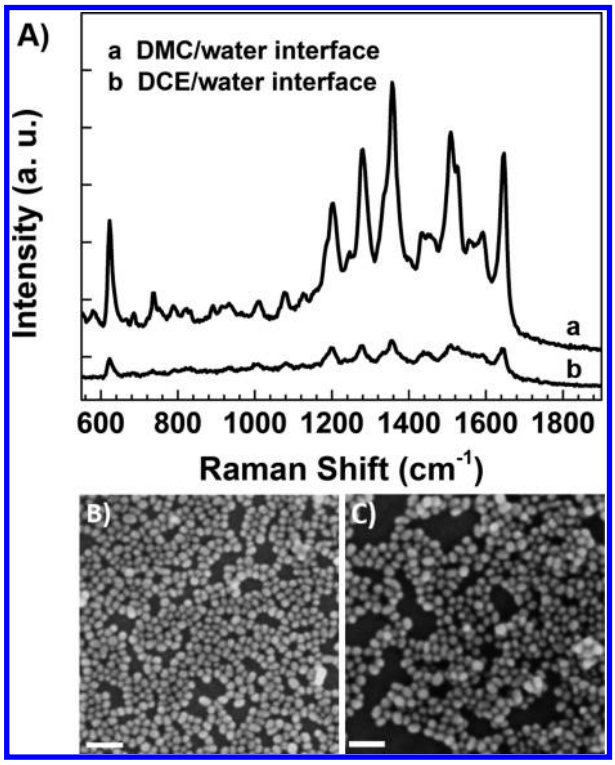

Figure 4. (A) Raman spectra on the surface of Au NP assemblies formed at (a) the DMC/water interface and (b) the DCE/water interface. 5 μM of R6G was used as the Raman reporter. SEM images of NP assemblies formed at (B) the DMC/water interface and (C) the DCE/water interface. Scale bars were 100 nm.

arranged NP monolayer was evidently observed at the DMC/water interface. The spatial uniformity of these arrays was considerably better than that in the case of the DCE/water interface (Figure 4C). The result of Raman measurements suggested that the NP arrays assembled at the DMC/water interface had stronger enhancement ability (Figure 4A). To further demonstrate the high affinity of the DMC/water interface for NPs location, UV−vis extinction spectroscopy was used to compare the extinction intensity change of Au NPs in the aqueous phase before and after assembly at the oil/liquid interface (Figure S2, Supporting Information). The extinction results were consistent with the SEM and Raman measurements. When DMC was used as the oil phase, the surface plasmon resonance intensity of Au NPs in aqueous phase after assembly was much weaker than that in the DCE/water system.

The volume ratio of DMC to water was varied to investigate the influence of the amount of DMC on NP assembly (Figure 5A). It was found that a ratio of 2:1 led to much stronger Raman signals. This was explained by the considerable effect of the DMC volume on the emulsifying efficiency. The amount of Au NPs is another important factor that directly affects the NP density and the interparticle distance within the assemblies. Spectra in Figure 5B suggested that 200 μL of 0.2 nM (1.1×10^{11} particles per milliliter) Au NPs resulted in the strongest Raman response.

These characterizations inspire us to explore such interfacial assembled NP arrays as a SERS sensor, namely, a sensor with both high sensitivity and specificity. However, it is well-known

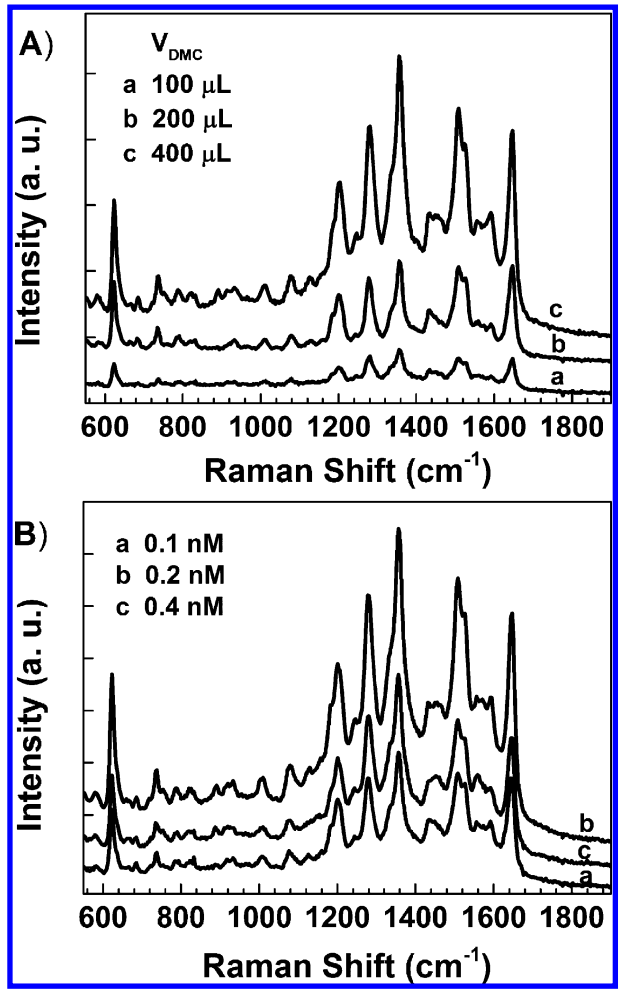

Figure 5. (A) Comparison of different DMC-to-water volume ratios. From top to bottom: the volume of DMC was (a) 100, (b) 200, and (c) 400 μL, corresponding to DMC-to-water volume ratios of 1:2, 1:1, and 2:1, respectively. (B) Comparison of different concentrations of Au NPs. The nanoparticle concentration was about (a) 0.1, (b) 0.2, and (c) 0.4 nM, respectively. 5 μM of R6G solution was used as the Raman reporter.

that citrate-stabilized Au NPs have no capability to selectively recognize target analytes. This issue could be resolved by introducing a specific chemical moiety onto the surfaces of Au NPs. In a proof-of-concept study, Au NPs were functionalized by cysteine to selectively detect trace TNT, a commonly used nitro-containing organic explosive. This compound was selected as a model analyte not only because of its potential safety hazard but also due to the spectral similarity between TNT and its structural analogues.[43,44]

Modifying Au NPs with cysteine allows for the specific recognition of TNT through a charge-transfer interaction between electron-rich amine ligands (donor) and electron-deficient aromatic rings (acceptor). The electron transfer from amino groups to aromatic rings results in the formation of a π-donor−acceptor complex (the so-called Meisenheimer complex).[45,46] It has been reported that high concentrations of cysteine could induce the aggregation of Au NPs primarily through electrostatic interactions between the charged amine and acid groups of cysteine molecules.[47] We used 10^{-8} M of cysteine in the present work and did not observe any aggregation, as experimentally documented by little change in

dx.doi.org/10.1021/ac501383x | Anal. Chem. 2014, 86, 6660−6665

the wavelength of the plasmon peak and the particle size distribution measured with both SEM and dynamic light scattering (DLS) (Figure S3, Supporting Information).

The selectivity and sensitivity of this system were inspected by adding various nitro-containing compounds into the cysteine-modified Au NPs solution. After self-assembly at the DMC/water interface, the SERS spectra were recorded from the surface of the NP arrays. As shown in Figure 6A, a

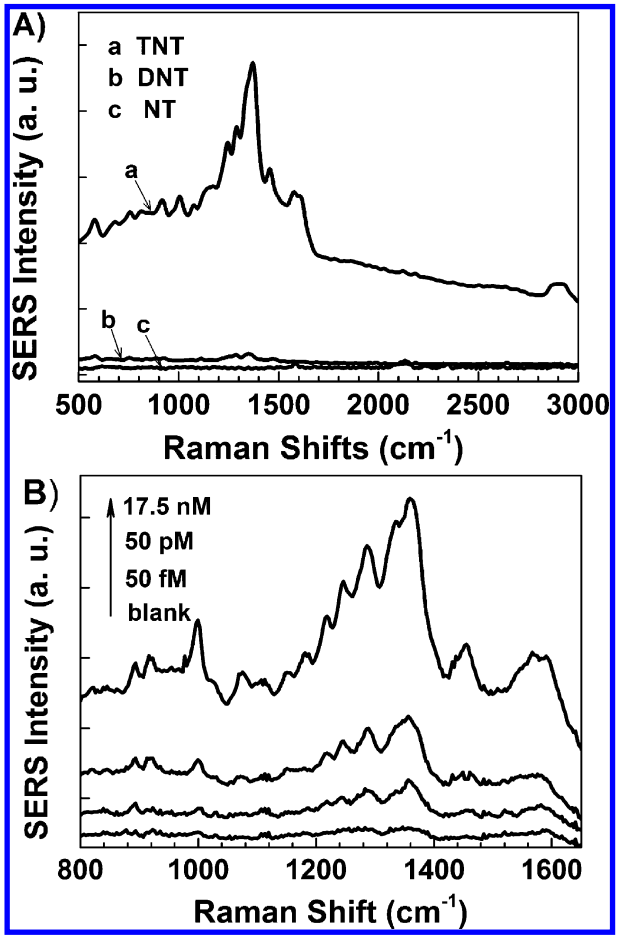

Figure 6. (A) SERS spectra of various nitro compounds obtained from the surface of NP self-assembled arrays. (B) SERS spectra showing a dilution series of TNT binding at the surface of cysteine-functionalized Au NP self-assemblies.

prominent SERS signal of the Meisenheimer complex could be obtained in the presence of TNT. The broadband at around 2900 cm^{-1} indicated the formation of the Meisenheimer complex corresponding to the NH_2^+ symmetric stretching, C–H stretching, and C–H_2 symmetric stretching. The two bands near 1600 cm^{-1} were due to ring stretching. The weak peak at 1536 cm^{-1} was ascribed to the NO_2 asymmetric stretching vibration, and the strong band at 1371 cm^{-1} was due to the NO_2 symmetric stretching vibration. The band at about 1000 cm^{-1} was assigned to ring breathing vibration.[48] The SERS spectra in Figure 6A also clearly indicated that 2,4-dinitrotoluene (DNT) and 3-nitrotoluene (NT), two structural analogues of TNT, had no SERS response on the surface of the interfacial NP assemblies. In the case of DNT, due to the lack of enough anionic charge throughout the molecular ring, DNT could not form the Meisenheimer complex, and as a result, binding to the surfaces of cysteine-Au NPs was prevented. The same mechanism could explain why NT was not attached to the surfaces of cysteine functionalized Au NPs.[49] Besides the good specificity, the liquid sensor also exhibited high sensitivity. As the SERS results show in Figure 6B, TNT as low as 50 fM was detectable. The sensitivity was superior to most of the reported results obtained from other SERS substrates,[3,43,44,46,49] demonstrating the effectiveness of this interfacial SERS sensor.

UV–vis extinction measurements were further used to confirm the interaction between TNT and cysteine-Au NPs. After addition of TNT into the Au NPs suspension, the plasmon band at 532 nm decreased accompanying the appearance of a new broadband from 600 to 900 nm, indicating the aggregation of Au NPs caused by TNT (Figure S4, Supporting Information). The extinction spectra changed with time and reached the maximum level within 30 s, suggesting very fast reaction kinetics between TNT and cysteine under the current experimental conditions (Figure S5, Supporting Information). We found that the pH value of the aqueous phase was about 5.5 after mixing TNT with cysteine-Au NPs. At this pH, cysteine remains in a state of electroneutrality. It has been reported that the reduction of the charge density on the Au nanoscrystals (NCs) is important for the formation of a NC monolayer at the oil/water interface.[50] In this sense, the presence of TNT may promote the location of NPs at the interface and in turn improve the sensitivity of TNT detection.

■ CONCLUSIONS

In conclusion, we have shown that the DMC/water interface is capable of organizing Au NPs into densely packed 2D assemblies. The resultant NP arrays on this template-free substrate enable the development of a highly sensitive SERS sensor for the rapid detection of trace analytes. Using DMC as the organic phase improves the efficiency of self-assembly and reduces the hazardous effects on the environment. The closely spaced NP arrays generate a large number of electromagnetic "hot spots". The unique assembly mechanism ensures that the dense assemblies are optically uniform. By incorporating specific functional ligands onto the surfaces of Au NPs, the direct and sensitive detection of specific target molecules in complex samples can be realized. This liquid sensor is easy-to-create and simple-to-use and thus opens new opportunities for trace detection of specific molecules in environmental samples.

■ ASSOCIATED CONTENT

Supporting Information

Details on FDTD calculations, SEM images on particle sizes, and supplementary figures. This material is available free of charge via the Internet at http://pubs.acs.org.

■ AUTHOR INFORMATION

Corresponding Author

*E-mail: bhliu@fudan.edu.cn.

Notes

The authors declare no competing financial interest.

■ ACKNOWLEDGMENTS

This work was supported by NSFC (21375022, 21175028, and 21105014).

■ REFERENCES

(1) Kneipp, K.; Kneipp, H.; Kneipp, J. *Acc. Chem. Res.* **2006**, *39*, 443–450.

(2) Constantino, C. J. L.; Lemma, T.; Antunes, P. A.; Aroca, R. *Anal. Chem.* **2001**, *73*, 3674−3678.
(3) Yang, L.; Ma, L.; Chen, G.; Liu, J.; Tian, Z. *Chem.—Eur. J.* **2010**, *16*, 12683−12693.
(4) Ngo, H. T.; Wang, H.-N.; Fales, A. M.; Vo-Dinh, T. *Anal. Chem.* **2013**, *85*, 6378−6383.
(5) Le, F.; Brandl, D. W.; Urzhumov, Y. A.; Wang, H.; Kundu, J.; Halas, N. J.; Aizpurua, J.; Nordlander, P. *ACS Nano* **2008**, *2*, 707−718.
(6) Tao, A.; Kim, F.; Hess, C.; Golberger, J.; He, R.; Sun, Y.; Xia, Y.; Yang, P. *Nano Lett.* **2003**, *3*, 1229−1233.
(7) Brolo, A. G.; Arctander, E.; Gordon, R.; Leathem, B.; Kavanagh, K. L. *Nano Lett.* **2004**, *4*, 2015−2018.
(8) Wang, H.; Levin, C. S.; Halas, N. J. *J. Am. Chem. Soc.* **2005**, *127*, 14992−14993.
(9) Li, J. F.; Huang, Y. F.; Ding, Y.; Yang, Z. L.; Li, S. B.; Zhou, X. S.; Fan, F. R.; Zhang, W.; Zhou, Z. Y.; Wu, D. Y.; Ren, B.; Wang, Z. L.; Tian, Z. Q. *Nature* **2010**, *464*, 392−395.
(10) Greeneltch, N. G.; Blaber, M. G.; Henry, A.-I.; Schatz, G. C.; Van Duyne, R. P. *Anal. Chem.* **2013**, *85*, 2297−2303.
(11) Van Duyne, R. P.; Hulteen, J. C.; Treichel, D. A. J. *Chem. Phys.* **1993**, *99*, 2101−2115.
(12) Grande, M.; Bianco, G. V.; Vincenti, M. A.; Stomeo, T.; deCeglia, D.; De Vittorio, M.; Petruzzelli, V.; Scalora, M.; Bruno, G.; D'Orazio, A. *Appl. Phys. Lett.* **2012**, *101*, 111606−111609.
(13) Gao, H. W.; Henzie, J.; Odom, T. W. *Nano Lett.* **2006**, *6*, 2104−2108.
(14) Li, S. H.; Bantz, K. C.; Lindquist, N. C.; Oh, S.-H.; Haynes, C. L. *Langmuir* **2009**, *25*, 13685−13693.
(15) Chen, A.; DePrince, A. E.; Demortière, A.; Joshi-Imre, A.; Shevchenko, E. V.; Gray, S. K.; Welp, U.; Vlasko-Vlasov, V. K. *Small* **2011**, *7*, 2365−2371.
(16) Fang, P.-P.; Chen, S.; Deng, H.; Scanlon, M. D.; Gumy, F.; Lee, H. J.; Momotenko, D.; Amstutz, V.; Cortés-Salazar, F.; Pereira, C. M.; Yang, Z.; Girault, H. H. *ACS Nano* **2013**, *7*, 9241−9248.
(17) Turek, V. A.; Cecchini, M. P.; Paget, J.; Kucernak, A. R.; Kornyshev, A. A.; Edel, J. B. *ACS Nano* **2012**, *6*, 7787−7799.
(18) Kim, K.; Han, H. S.; Choi, I.; Lee, C.; Hong, S.; Suh, S.-H.; Lee, L.-P.; Kang, T. *Nat. Commun.* **2013**, *4*, 2182.
(19) Schaming, D.; Hojeij, M.; Younan, N.; Nagatani, H.; Lee, H. J.; Girault, H. H. *Phys. Chem. Chem. Phys.* **2011**, *13*, 17704−17711.
(20) Su, B.; Abid, J.-P.; Fermín, D. J.; Girault, H. H.; Hoffmannová, H.; Krtil, P.; Samec, Z. *J. Am. Chem. Soc.* **2004**, *126*, 915−919.
(21) Liu, J.-W.; Zhang, S.-Y.; Qi, H.; Wen, W.-C.; Yu, S.-H. *Small* **2012**, *8*, 2412−2420.
(22) Turek, V. A.; Elliott, L. N.; Tyler, A. I. I.; Demetriadou, A.; Paget, J.; Cecchini, M. P.; Kucernak, A. R.; Kornyshev, A. A.; Edel, J. B. *ACS Nano* **2013**, *7*, 8753−8759.
(23) Cecchini, M. P.; Turek, V. A.; Paget, J.; Kornyshev, A. A.; Edel, J. B. *Nat. Mater.* **2013**, *12*, 165−171.
(24) Konrad, M. P.; Doherty, A. P.; Bell, S. E. J. *Anal. Chem.* **2013**, *85*, 6783−6789.
(25) Frens, G. *Nat. Phys. Sci.* **1973**, *241*, 20−22.
(26) Liu, X.; Atwater, M.; Wang, J.; Huo, Q. *Colloids Surf., B* **2007**, *58*, 3−7.
(27) Binks, B. P. *Curr. Opin. Colloids Interface Sci.* **2002**, *7*, 21−24.
(28) Birdi, K. S., Ed. *Handbook of Surface and Colloid Chemistry*, 3rd ed.; CRC Press: Boca Roton, FL, 2009.
(29) Reincke, F.; Hickey, S. G.; Kegel, W. K.; Vanmaekelbergh, D. *Angew. Chem., Int. Ed.* **2004**, *43*, 458−462.
(30) Duan, H.; Wang, D.; Kurth, D. G.; Möhwald, H. *Angew. Chem., Int. Ed.* **2004**, *43*, 5639−5642.
(31) Yang, Z.; Chen, S.; Fang, P.; Ren, B.; Girault, H. H.; Tian, Z. *Phys. Chem. Chem. Phys.* **2013**, *15*, 5374−5378.
(32) Hojeij, M.; Younan, N.; Ribeaucourt, L.; Girault, H. H. *Nanoscale* **2010**, *2*, 1665−1669.
(33) Michaels, A. M.; Nirmal, M.; Brus, L. E. *J. Am. Chem. Soc.* **1999**, *121*, 9932−9939.
(34) Lee, W.; Lee, S. Y.; Brider, R. M.; Rabin, O. *Adv. Funct. Mater.* **2011**, *21*, 3424−3429.
(35) Zheng, Y.; Thai, T.; Reineck, P.; Qiu, L.; Guo, Y.; Bach, U. *Adv. Funct. Mater.* **2013**, *23*, 1519−1526.
(36) Lee, C. H.; Hankus, M. E.; Tian, L.; Pellegrino, P. M.; Singamaneni, S. *Anal. Chem.* **2011**, *83*, 8953−8958.
(37) Que, R.; Shao, M.; Zhuo, S.; Wen, C.; Wang, S.; Lee, S.-T. *Small* **2011**, *21*, 3337−3343.
(38) Cho, W. J.; Kim, Y.; Kim, J. K. *ACS Nano* **2012**, *6*, 249−255.
(39) Tanoue, Y.; Sugawa, K.; Yamamuro, T.; Akiyama, T. *Phys. Chem. Chem. Phys.* **2013**, *15*, 15802−15805.
(40) Tundo, P.; Selva, M. *Acc. Chem. Res.* **2002**, *375*, 706−716.
(41) Tundo, P. *Pure Appl. Chem.* **2001**, *73*, 1117−1124.
(42) Fang, A.; Gaillard, C.; Douliez, J.-P. *Chem. Mater.* **2011**, *23*, 4660−4662.
(43) Kanchanapally, R.; Sinha, S. S.; Fan, Z.; Dubey, M.; Zakar, E.; Ray, P. C. *J. Phys. Chem. C* **2014**, *118*, 7070−7075.
(44) Liu, X.; Zhao, L.; Shen, H.; Xu, H.; Lu, L. *Talanta* **2011**, *83*, 1023−1029.
(45) Gao, D.; Wang, Z.; Liu, B.; Ni, L.; Wu, M.; Zhang, Z. *Anal. Chem.* **2008**, *80*, 8545−8553.
(46) Wang, J.; Yang, L.; Liu, B.; Jiang, H.; Liu, R.; Yang, J.; Han, G.; Mei, Q.; Zhang, Z. *Anal. Chem.* **2014**, *86*, 3338−3345.
(47) Mocanu, A.; Cernica, I.; Tomoaia, G.; Bobos, L. D.; Horovitz, O.; Tomoaia-Cotisel, M. *Colloids Surf., A* **2009**, *338*, 93−101.
(48) Kneipp, K.; Wang, Y.; Dasari, R. R.; Feld, M. S.; Gilbert, B. D.; Janni, J.; Steinfeld, J. I. *Spectrochim. Acta, Part A* **1995**, *51*, 2171−2175.
(49) Dasary, S. S. R.; Singh, A. K.; Senapati, D.; Yu, H.; Ray, P. C. *J. Am. Chem. Soc.* **2009**, *131*, 13806−13812.
(50) Reincke, F.; Kegel, W. K.; Zhang, H.; Nolte, M.; Wang, D.; Vanmaekelbergh, D.; Möhwald, H. *Phys. Chem. Chem. Phys.* **2006**, *8*, 3828−3835.